PERGAMON

International Journal of Heat and Mass Transfer 44 (2001) 3125–3134

International Journal of HEAT and MASS TRANSFER

www.elsevier.com/locate/ijhmt

Interfacial electrokinetic effects on liquid flow in microchannels

Liqing Ren, Weilin Qu, Dongqing Li *

Department of Mechanical & Industrial Engineering, University of Toronto, 5 King's College Road, Toronto, Ont., Canada M5S 3G8

Received 11 May 2000; received in revised form 9 October 2000

Abstract

The presence of the electrical double layer near a solid–liquid interface results in the electro-viscous effect on pressure-driven liquid flow through microchannels. The objective of this paper is to examine the magnitude of the additional flow resistance caused by the electrokinetic effect in microchannels. De-ionized ultra-filtered water and aqueous KCl solutions of two different concentrations (10^{-4} and 10^{-2} M) were used as the testing liquids. Carefully designed flow measurements were conducted in three silicon microchannels with a height of 14.1, 28.2 and 40.5 μm, respectively. The measured dP/dx for the pure water and the low concentration solution were found to be significantly higher than that without electro-viscous effect at the same Reynolds number. Such a difference strongly depends on the channel's height and the ionic concentration of the liquids. The flow-induced streaming potential was also measured and the data confirm a higher electro-viscous effect on the flow of pure water and low concentration KCl solution. The experimental results were compared with the predictions of a theoretical electro-viscous flow model, and a good agreement was found. © 2001 Elsevier Science Ltd. All rights reserved.

1. Introduction

Due to the rapid development of Micro-Electro-Mechanical Systems (MEMS) and microfluidics such as microchannel heat sinks for cooling micro-chips and laser diode arrays, Lab-On-Chip devices for chemical and biomedical analyses, and micro fluid pumps, etc., it is highly desirable to understand the fundamental characteristics of liquid flow in microchannels. However, because of the influence of the solid (channel wall)–liquid interfaces, the flow behavior in microchannels often deviates from the prediction of the traditional form of the Navier–Stokes (NS) equation.

Tuckerman and Pease [1] employed rectangular microchannels as high-performance heat sinks for cooling electronic components. They found that the experimental results of flow friction were slightly higher than those predicted by classical theories. Several other investigators confirmed this similar, anomalous behavior for microchannel flow in their studies. Rahman and Gui [2] measured water flow in silicon microchannels with different ratios of height to width. Their results showed that the friction coefficient has the same pattern as Tuckerman's results. Urbanek et al. [3] investigated liquid (1,2-propanol and 1,3-pentanol) flow through 5, 12, and 25 μm hydraulic diameter microchannels with liquid temperature varying from 0°C to 85°C. The friction coefficient dependence on fluid temperature and the channel size was reported. Pfahler [4] has measured the friction coefficient in microchannels. Non-conventional flow behavior was observed for both isopropanol and silicon oil. His results indicate that polar fluids (isopropanol) and non-polar fluids (silicon oil) behave differently, and that polar nature of the fluid may play a role in the microchannel flow. An experimental study by Mala et al. [5] showed that the flow behavior of water and electrolyte solutions in glass and silicon microchannel depends on channel material, channel size and liquid properties. Mala and Li [6] also showed that the pressure drop of water flow through microtubes is significantly higher than that predicted by the conventional theory. Under the same flow rate and for the same diameter, the pressure drop in metal tubes is lower than that in silica glass tubes. Generally, the experimental

* Corresponding author. Tel.: +1-416-978-1282; fax: +1-416-978-7753.

E-mail address: dli@mie.utoronto.ca (D. Li).

0017-9310/01/$ - see front matter © 2001 Elsevier Science Ltd. All rights reserved.
PII: S0017-9310(00)00339-2

Nomenclature

D_h	hydraulic diameter, m
EDL	electrical double layer
E_x	streaming potential, V/m
H	half channel height, m
L	channel length, m
I_c, I_s	conduction and streaming current, respectively, A
P	hydraulic pressure in x-direction
Q	volumetric flow rate, m^3/s
Re	Reynolds number
T	absolute temperature, K
U	reference velocity, m/s
W	half channel width, m
e	charge of a proton, C
k_b	Boltzmann constant, J/mol K
n_+, n_-	concentration of positive and negative ions, m^{-3}
n_∞	bulk concentration of ions, m^{-3}
u	liquid velocity component in x flow direction, m/s
u_m	mean liquid velocity component in x flow direction, m/s
x^*	non-dimensional x-coordinate
y^*	non-dimensional y-coordinate
z^*	non-dimensional z-coordinate
z_+, z_-	valence of the positive and negative ions

Greek symbols

ε	absolute dielectric constant of the fluid, c/V m
κ	Debye–Hückel parameter, m^{-1}
λ_0	bulk electrical conductivity $(1/\Omega\ m)$
μ	dynamic viscosity of the liquid, kg/m s
ρ_e	local net electric charge density, c/m^3
ρ	density of the fluid, kg/m^3
ς	Zeta potential, V
ψ	local electrostatic potential in the EDL, V

data of friction coefficient and apparent viscosity in these previous investigations are contrary to the conventional theories. The smaller the channels, the larger the differences.

One possible explanation for these unusual behaviors of the microchannel flow is the interfacial electrokinetic or the electro-viscous effect. It is known that most solid surfaces have electrostatic charges, i.e., an electrical surface potential. If the liquid contains a very small number of ions (for instance, due to impurities), the electrostatic charges on the non-conducting solid surface will attract the counterions in the liquid. The rearrangement of the charges on the solid surface and the balancing charges in the liquid is called the electrical double layer (EDL) [7]. Because of the electrostatic interaction, the counterion concentration near the solid surface is higher than that in the bulk liquid far away from the solid surface. Immediately next to the solid surface, there is a layer of ions that are strongly attracted to the solid surface and are immobile. This layer is called the compact layer, normally less than 1 nm thick. From the compact layer to the uniform bulk liquid, the counterion concentration gradually reduces to that of bulk liquid. Ions in this region are affected less by the electrostatic interaction and are mobile. This layer is called the diffuse layer of the EDL. The thickness of the diffuse layer depends on the bulk ionic concentration and electrical properties of the liquid, ranging from a few nanometers for high ionic concentration solutions up to several micrometers for distilled water and pure organic liquids. The boundary between the compact layer and the diffuse layer is usually referred to as the shear plane. The electrical potential at the solid–liquid surface is difficult to measure directly. The electrical potential at the shear plane, however, is called the Zeta potential, ζ, is a property of the solid–liquid pair, and can be measured experimentally [7].

When a liquid is forced through a microchannel under an applied hydrostatic pressure, the counterions in the diffuse layer (mobile part) of the EDL are carried towards the downstream end, resulting in an electrical current in the pressure-driven flow direction. This current is called the streaming current. Corresponding to this streaming current, there is an electrokinetic potential called the streaming potential. This flow-induced streaming potential is a potential difference that builds up along a microchannel. This streaming potential acts to drive the counterions in the diffuse layer of the EDL to move in the direction opposite to the streaming current, i.e., opposite to the pressure-driven flow direction. The action of the streaming potential will generate an electrical current called the conduction current. It is obvious that when ions move in a liquid, they will pull the liquid molecules to move with them. Therefore, the conduction current will produce a liquid flow in the opposite direction to the pressure-driven flow. The overall result is a reduced flow rate in the pressure drop direction. If the reduced flow rate is compared with the flow rate predicted by the conventional fluid mechanics theory without considering the presence of the EDL, it seems that the liquid would have a higher viscosity. This is usually referred to as the electro-viscous effect [7].

Generally, for macrochannel flow the EDL effects can be safely neglected, as the thickness of the EDL is

very small compared with the characteristic size of channels. However, for dilute electrolyte solutions flowing in microchannels, the thickness of the EDL may be comparable with the characteristic size of flow channels. Thus the electro-viscous effect described above should be considered. Because the electro-viscous effect originates from the EDL field which in turn depends on the material of the channel wall, the size and shape of the channel, and the ionic concentration, dielectric constant and other properties of the liquid, it is not difficult to understand that microchannel flow may depend on the liquid and on the material and size of the channel, as reported in the literature.

In the literature there are some theoretical models considering the EDL effects on microchannel flow characteristics. Burgreen and Nakache [8] studied the effect of the surface potential on liquid transport through fine capillary slits by using an approximation valid only for cases of low surface potentials. Rice and Whitehead [9] discussed the same problem in narrow cylindrical capillaries. Levine et al. [10] extended Rice and Whitehead's model for cylindrical capillaries to a higher surface potential by developing an approximate solution. In practice, microchannels used in microfluidic devices are made by modern micromachining technology. The cross-section of these microchannels is close to a rectangular shape. In such a situation, the two-dimensional channel cross-section shape and especially the corner of the channel have important contribution to the EDL field, subsequently to the flow field. A recent model developed by Yang et al. [11–13] revealed significant electro-viscous effects on liquid flow in rectangular microchannels in terms of the aspect ratio of the channel's cross-section, the surface potential and the ionic concentration.

A key question: Is the interfacial electro-viscous effect as large as predicted by these theoretical models? So far there has been no direct experimental verification to these models. The objectives of this paper are to examine if the electro-viscous effect can be measured, and to compare the measured effect with the theoretical model prediction. To do so, careful experimental studies were conducted. If non-conventional flow behavior is due to the interfacial electrokinetic or electro-viscous effects, it must depend on the ionic concentrations of the testing liquid. For this purpose, pure water and aqueous KCl solutions of two different concentrations were chosen as the testing liquids. It was found that micromachined channels on glass or silicon plates have a trapezoidal cross-section and relatively rough surface [14]. To avoid the complication due to cross-section geometry and the surface roughness of the flow channels, microchannels formed by two parallel, smooth silicon plates were used in our studies. The experimental data show significant electro-viscous effect and were compared with an electrokinetic flow model.

2. Experimental

Fig. 1 shows the experimental system used to study the electrokinetic effect on the flow characteristics of a liquid flowing through a microchannel. This system consists of a flow loop, a test section including a slit microchannel, instruments for measuring flow and electrokinetic parameters, and a computer data acquisition system.

De-ionized ultra-filtered water (DIUF) (Fisher Scientific) and aqueous KCl solutions of two different concentrations were used as the testing liquids. The concentrations of the KCl solutions are 10^{-4} and 10^{-2} M (kmol/m^3), respectively. In the experiments, the testing liquid was pumped from a liquid reservoir to the flow loop by a high precision displacement pump (Ruska Instruments, Model: 2248-WII) which has a flow rate range of 2.5–560 cm^3/h and can generate a pressure up to 4000 psi (27.6 MPa). A 0.1 μm filter was installed in the flow loop between the outlet of the pump and the inlet of the test section. The liquid was forced to flow through this submicron filter before entering the test section to avoid any particles or bubbles from flowing through the test section and blocking the microchannel. In order to minimize the environmental electrical interference on the measurement of the electrokinetic parameters, such as the streaming potential across the microchannel and the bulk conductivity of the liquid, the whole flow loop is made of plastic tubes and plastic valves.

The silicon plates (30 mm in length, 14 mm in width and 1 mm in thickness) used to form the microchannels in this study were supplied by Alberta Microelectronic Center (Edmonton, Canada). The surface roughness of these plates is approximately 20 nm. To form a microchannel, first two strips of a thin plastic shim (Small Parts Inc.) were used as the spacer and put between a

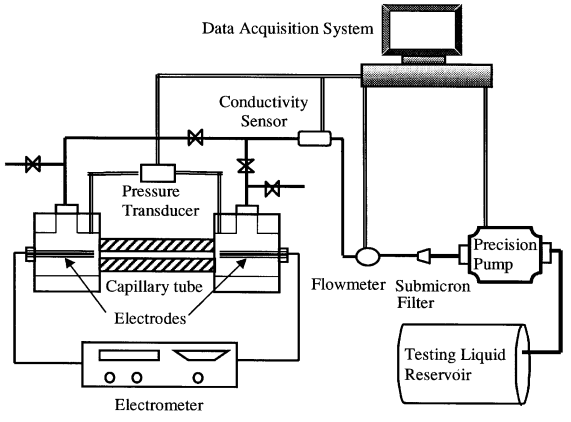

Fig. 1. Schematic of the experimental system used to measure the flow in microchannels.

pair of silicon plates in the length direction along the sides of the plates, so that a flow passage of 5 mm width was formed. Then, a specially designed clapper was used to fix the relative position of the plates and the thin spacers. Finally, epoxy resin was applied to bond the clapper and the silicon plates together and to seal all the openings except the inlet and outlet of the microchannel. The cross-section of such a microchannel is illustrated in Fig. 2. Three microchannels were made in this way and tested in this study. The channels have identical width and length which are 5 and 30 mm, respectively, and different heights. By choosing different shim thicknesses, the heights of the three microchannels are 14.1, 28.2 and 40.5 μm, respectively. The width and length of the microchannel can be accurately measured by using a precision gauge. The height of the microchannels was first directly measured by a microscope (Leica MS5 Stereomicroscope) – computer image analysis system with a resolution of 0.8 μm. Then the channel height was calibrated by an indirect method that involves the flow of a high ionic concentration solution through the microchannel. For a high concentration electrolyte solution, the EDL thickness is very small (about a few nanometers) and the electrokinetic effect on the flow is negligible. The liquid flow in such a case is basically a Poiseuille laminar flow. Therefore, the channel height can be determined from the measured pressure drop and flow rate by using the Poiseuille flow equation. The channel heights determined in this way were used in this study. It was found that the difference between the measured channel heights from these two methods was less than 0.5 μm.

A microchannel was placed in a two-part symmetrical Plexiglas assembly to form a test section, as shown in Fig. 1. The epoxy resin was applied to bond the microchannel and the assembly together to avoid leaking. It was found that the height of the microchannel may be altered if the pressure of the liquid in the microchannel was too high. This is because neither the clapper nor the epoxy resin can stand very high pressure and deformation may happen. This limited our experiments to a small Reynolds number range especially for smaller microchannels.

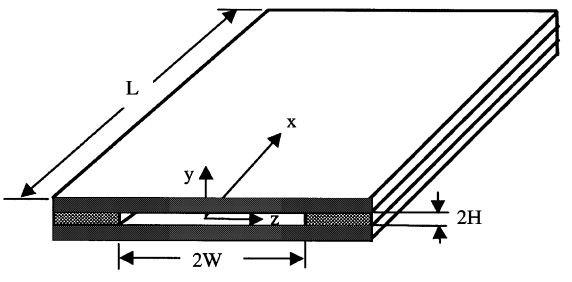

Fig. 2. Illustration of the microchannel formed between two parallel silicon plates.

Two pairs of sumps were machined in the assembly and were used for the pressure drop and streaming potential measurement. A diaphragm type differential pressure transducer (Validyne Engineering, Model: DP15) with ±0.5% FS accuracy was connected to one pair of sumps to measure the pressure drop along the microchannel. The pressure transducer was calibrated by using a standard deadweight pressure source before being used in the experiments. The details of the calibration procedures and the results can be found elsewhere [15]. The flow-induced electrokinetic potential, the streaming potential, was measured by a pair of Ag/AgCl electrodes (Sensortechnik Meinsberg GmbH) and an electrometer (Keithley Instruments, Model 6517).

The volume flow rate of water flowing through the microchannels was measured by the weighting method as described below. The liquid exiting the test section was accumulated in a glass beaker whose weight was measured before. A stopwatch was employed to measure the time spent for the accumulation. Then, an electronic balance (Mettler Instrument AG, model: BB240) with an accuracy of 0.001 gram was used to measure the weight of the accumulated liquid. Usually one to two grams of the liquid was collected over approximately 20–30 min depending on the channel size and the flow rate. Evaporation effect was examined and found to be negligible. The total volume of the liquid was determined by dividing the weight by the liquid's density. The flow rate was then obtained by dividing the total volume of the accumulated liquid by the time. The accuracy of the flow rate measurement was estimated to be ±2%.

In an experiment, the pump was set to maintain a constant flow rate. The readings of the pressure drop along the microchannel were monitored and recorded. The flow was considered to have reached a steady state when the readings of the pressure drop did not change any more. The data reported in this paper are for steady-state flow. For a given channel and a given testing liquid, the measurements for all the parameters were repeated at least twice for the same flow rate and in the same flow direction. The flow direction was then switched by adjusting the control valves, and the measurements were conducted for the same flow rate after the steady state was reached. Again, the measurements were repeated at least twice. After the measurements for both the flow directions were completed, the pump was set to a different flow rate and the measurements described above were repeated for the same microchannel, and so on.

When changing a different testing liquid, the flow loop and the test section were flushed thoroughly by DIUF water and then the testing liquid for several hours to remove all the ions and/or other possible contamination left from the previous test. Because the electrical conductivity of the liquid is very sensitive to an even very small change in the ionic concentration, an on-line electrical conductivity sensor (Model:CR 7300,

Metter-Toledo Process Analytical) was used as a monitor. The flushing process was continued until a steady liquid conductivity reading was achieved and was the same as the standard value for that liquid.

Consider a rectangular microchannel of width $2W$, height $2H$ and length L, as illustrated in Fig. 2. In the entrance region, the liquid flow was not fully developed laminar flow. The entrance region length is given by [16]

$$L_{\text{in}} = 0.02(2H)Re \quad \left(Re = \frac{\rho u_{\text{m}} D_{\text{h}}}{\mu}\right), \tag{1}$$

where $D_{\text{h}} = 4HW/(H+W)$ is the hydraulic diameter of the rectangular channel, and u_{m} is the mean velocity. In this region, the pressure drop is calculated by

$$\Delta P_{\text{in}} = \frac{k_{\text{in}} \cdot \rho \cdot L_{\text{in}}}{2D_{\text{h}}} u_{\text{m}}^2, \tag{2}$$

where k_{in} is the friction coefficient given by [16]

$$k_{\text{in}} = \frac{96}{Re} + \frac{1}{Re}\left[\frac{0.774}{[L_{\text{in}}/2(2H)Re]} - \frac{0.00089}{[L_{\text{in}}/2(2H)Re]^2}\right]. \tag{3}$$

At the exit of the flow, the cross-section is greatly increased as the liquid leaves the slit microchannel and enters a big channel (about 10 mm in diameter). The liquid flow becomes turbulent. The pressure loss at the exit is estimated by

$$\Delta P_{\text{out}} = \frac{\rho}{2} u_{\text{m}}^2. \tag{4}$$

The net pressure drop without the losses at the entrance and at the exit is then

$$\Delta P_{\text{net}} = \Delta P_{\text{measured}} - \Delta P_{\text{in}} - \Delta P_{\text{out}}. \tag{5}$$

The pressure drop reported in this paper is the net pressure drop.

3. Theoretical electro-viscous flow model

3.1. Electrical double layer (EDL) in a rectangular microchannel

According to the theory of electrostatics, the relationship between the electrical potential, ψ, and the net charge density per unit volume, ρ_{e}, at any point in the liquid is described by the two-dimensional Poisson equation

$$\frac{\partial^2 \psi}{\partial y^2} + \frac{\partial^2 \psi}{\partial z^2} = -\frac{\rho_{\text{e}}}{\varepsilon_0 \varepsilon}, \tag{6}$$

where ε is the dielectric constant of the solution and ε_0 is the permittivity of vacuum. Assuming that the equilibrium Boltzmann distribution is applicable, which implies uniform dielectric constant and neglect of fluctuation, the number of ion distribution in a symmetric electrolyte solution is of the form

$$n_i = n_{i\infty} \exp\left(-\frac{z_i e \psi}{k_{\text{b}} T}\right), \tag{7}$$

where $n_{i\infty}$ and z_i are the bulk ionic concentration and the valence of type i ions, respectively, e the charge of a proton, k_{b} the Boltzmann's constant and T is the absolute temperature. The net volume charge density ρ_{e} is proportional to the concentration difference between cations and anions, via

$$\rho_{\text{e}} = ze(n_+ - n_-) = -2zen_\infty \sinh\left(\frac{ze\psi}{k_{\text{b}} T}\right). \tag{8}$$

Substituting Eq. (8) into the Poisson equation, the well-known Poisson–Boltzmann equation is obtained

$$\frac{\partial^2 \psi}{\partial y^2} + \frac{\partial^2 \psi}{\partial z^2} = \frac{2n_\infty ze}{\varepsilon \varepsilon_0} \sinh\left(\frac{ze\psi}{k_{\text{b}} T}\right). \tag{9}$$

By defining the Debye–Hückel parameter as $k^2 = 2z^2 e^2 n_\infty / \varepsilon \varepsilon_0 k_{\text{b}} T$ ($1/k$ is normally referred to as the EDL thickness), the hydraulic diameter of the rectangular microchannel as

$$D_{\text{h}} = 4HW/(H+W)$$

and introducing the dimensionless variables:

$$y^* = y/D_{\text{h}}, \qquad z^* = z/D_{\text{h}} \quad \text{and} \quad \psi^* = ze\psi/k_{\text{b}} T,$$

the above equation can be non-dimensionalized as

$$\frac{\partial^2 \psi^*}{\partial y^{*2}} + \frac{\partial^2 \psi^*}{\partial z^{*2}} = k^2 D_{\text{h}}^2 \sinh(\psi^*). \tag{10}$$

Because of symmetry of the EDL in a rectangular channel, Eq. (10) is subjected to the following boundary conditions in a quarter of the rectangular cross-section:

$$y^* = 0, \quad \frac{\partial \psi^*}{\partial y^*} = 0, \quad y^* = \frac{H}{D_{\text{h}}}, \quad \psi^* = \frac{ze\varsigma}{k_{\text{b}} T}, \tag{11a}$$

$$z^* = 0, \quad \frac{\partial \psi^*}{\partial z^*} = 0, \quad z^* = \frac{W}{D_{\text{h}}}, \quad \psi^* = \frac{ze\varsigma}{k_{\text{b}} T}, \tag{11b}$$

where the Zeta potential ς is a measurable electrical potential at the shear plane, i.e., the boundary between the compact layer and the diffuse layer of the EDL.

3.2. Flow field in a rectangular microchannel

The general equation of motion for laminar conditions in a liquid with constant density and viscosity is given by

$$\rho \frac{\partial \overline{u}}{\partial t} + \rho \overline{u} \cdot \nabla \overline{u} = -\nabla P + \mu \nabla^2 \overline{u} + \overline{F}. \tag{12}$$

Assuming the flow is steady, two-dimensional, and fully developed, the velocity components satisfy $u = u(y,z)$

and $v = w = 0$. Then both the time term, $\partial\overline{u}/\partial t$, and the inertia term, $\overline{u} \cdot \nabla\overline{u}$, vanish. Also, the hydraulic pressure P is a function of x only and the pressure gradient, $\mathrm{d}P/\mathrm{d}x$, is constant. If the gravity effect is negligible, the body force, $\overline{F}$, is only from an induced electrical field, E_x. Under the above conditions, the general equation of motion is reduced to

$$\frac{\partial^2 u}{\partial y^2} + \frac{\partial^2 u}{\partial z^2} = \frac{1}{\mu}\frac{\mathrm{d}P}{\mathrm{d}x} - \frac{1}{\mu}E_x\rho_e \tag{13}$$

In Eq. (13), the electrokinetic potential E_x can be obtained through the balance between streaming current and electrical conduction current at the steady state. At a steady state, the net electrical current should be zero, which means

$$I = I_s + I_c = 0. \tag{14}$$

Because of symmetry, the electrical streaming current, transport of the net charge in the EDL region with the liquid flow, is given by

$$I_s = 4\int_0^H \int_0^W u(y,z)\rho_e(y,z)\,\mathrm{d}y\,\mathrm{d}z. \tag{15}$$

Realizing that the net charge density is non-zero essentially only in the EDL region whose characteristic thickness is given by $1/k$ (k is the Debye–Hückel parameter as defined previously), the lower boundary of the above integration may be changed to $(H - 1/k)$ and $(W - 1/k)$ instead of 0. That is,

$$I_s = 4\int_{H-1/k}^H \int_{W-1/k}^W u(y,z)\rho_e(y,z)\,\mathrm{d}y\,\mathrm{d}z. \tag{16}$$

The conduction current, the transport of the excess charge in the EDL region driven by the electrokinetic potential, is given by

$$I_c = \lambda_0 E_x A_c, \tag{17}$$

where λ_0 is the electrical conductivity of the liquid, and A_c is the cross-sectional area of the channel. Once again, since the net charge density is essentially zero outside of the EDL region whose characteristic thickness is given by $1/k$, the effective area of the rectangular channel's cross-section for the conduction current is approximately

$$A = 2\left(2W\frac{1}{k} + 2H\frac{1}{k}\right) = 4(W+H)\frac{1}{k}.$$

So the conduction current in the rectangular channel can be expressed as

$$I_c = 4\lambda_0 E_x (W+H)\frac{1}{k}. \tag{18}$$

Putting Eqs. (16) and (18) into the steady-state condition, Eq. (14) gives

$$E_x = -\frac{\int_{H-1/k}^H \int_{W-1/k}^W u(y,z)\rho_e(y,z)\,\mathrm{d}y\,\mathrm{d}z}{\lambda_0(W+H)(1/k)} \tag{19}$$

Substituting Eq. (19) for E_x and Eq. (8) for ρ_e into Eq. (13) and employing the following non-dimensional parameters:

$$y^* = \frac{y}{D_h}, \quad z^* = \frac{z}{D_h}, \quad x^* = \frac{x}{\rho D_h^2 U/\mu},$$
$$u^* = \frac{u}{U}, \quad P^* = \frac{P - P_0}{\rho U^2}, \quad M = \frac{4z^2 e^2 n_\infty^2 D_h^4}{\mu\lambda_0(W+H)(1/k)},$$

where U is a reference velocity, and P_0 is a reference pressure, then the following non-dimensional equation of motion can be obtained

$$\frac{\partial^2 u^*}{\partial y^{*2}} + \frac{\partial^2 u^*}{\partial z^{*2}} = \frac{\mathrm{d}P^*}{\mathrm{d}x^*} + M\sinh(\psi^*)\int_{H/D_h - 1/kD_h}^{H/D_h} \times \int_{W/D_h - 1/kD_h}^{W/D_h} u^*\sinh(\psi^*)\,\mathrm{d}y^*\,\mathrm{d}z^*. \tag{20}$$

The above equation of motion is subjected to the following boundary conditions:

$$y^* = 0, \quad \frac{\partial u^*}{\partial y^*} = 0, \qquad y^* = \frac{H}{D_h}, \quad u^* = 0, \tag{21a}$$

$$z^* = 0, \quad \frac{\partial u^*}{\partial z^*} = 0, \qquad z^* = \frac{W}{D_h}, \quad u^* = 0. \tag{21b}$$

Numerically solving the Poisson–Boltzmann equation, Eq. (10), and the equation of motion, Eq. (20), with the boundary conditions specified in Eqs. (11a), (11b), and (21a), (21b), both the EDL field and the velocity field in the rectangular microchannel can be determined. The EDL or electrokinetic effects on the flow characteristics such as the $\mathrm{d}P/\mathrm{d}x$ vs. Re relationship can be predicted.

4. Results and discussions

Using the measured flow rate, Q, and the measured pressure drop, the pressure gradient and the Reynolds number are calculated as follows:

$$\frac{\mathrm{d}P}{\mathrm{d}x} = \frac{\Delta P_{net}}{L}, \tag{22}$$

$$\mathrm{Re} = \frac{\rho Q D_h}{\mu A_c}, \tag{23}$$

where ΔP_{net} is determined from Eq. (5), L is the length of the channel (30 mm), D_h the hydraulic diameter of the channel, and A_c is the cross-sectional area of the channel. For the microchannels of three different heights, the experimentally determined pressure gradient and the Reynolds numbers were plotted in Figs. 3–5. Generally, for a given liquid, there are six data points for one and approximately the same Reynolds number. All data reported in this paper are at 21°C.

For KCl solution at the high concentration 10^{-2} M (i.e., kmol/m^3), the EDL thickness is approximately

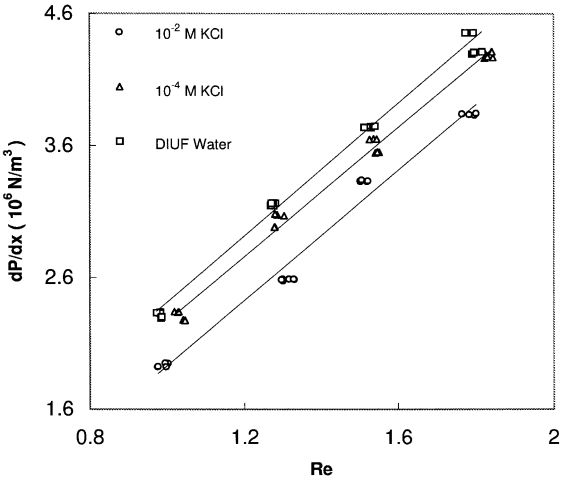

Fig. 3. Experimentally determined pressure gradient and Reynolds number for a microchannel of height 14.1 μm.

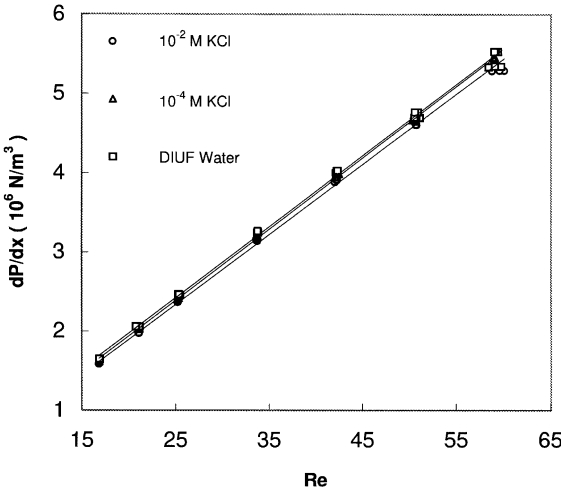

Fig. 5. Experimentally determined pressure gradient and Reynolds number for a microchannel of height 40.5 μm.

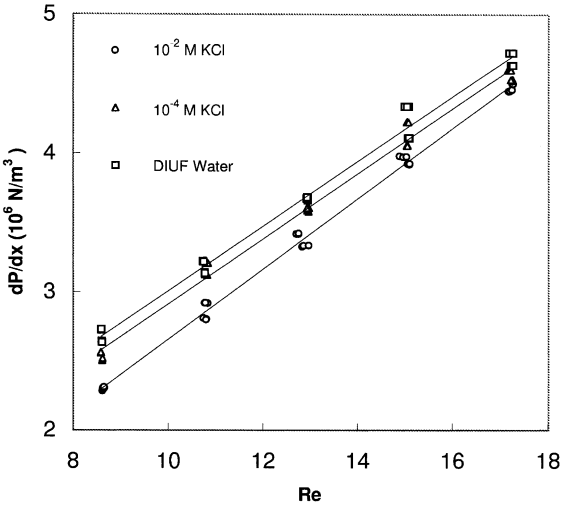

Fig. 4. Experimentally determined pressure gradient and Reynolds number for a microchannel of height 28.2 μm.

several nanometers. The EDL effect on flow can be neglected as the EDL thickness is so small in comparison with the channel height. The flow in the microchannels is considered as the conventional Poiseuille laminar flow. However, the EDL thickness is approximately 100 nm for the 10^{-4} M solution and 1 μm for the DIUF water, respectively. As seen clearly from all these figures, for the lower concentration (10^{-4} M) solution and the pure water, the measured pressure gradients at the same Reynolds number (i.e., the same flow rate) are significantly (up to 20%) higher than that for the high concentration solution where there is no EDL effect on flow. However, the difference in dP/dx between the pure water and the 10^{-2} M solution diminishes as the channel height increases. Furthermore, for all the three microchannels, there are clear differences between the $dP/dx \sim Re$ relationships for the 10^{-4} M solution and that for the pure water. That is, at the same Reynolds number, the dP/dx for the pure water is always higher than that of the 10^{-4} M solution. These experimental results show a strong dependence of the flow characteristics in microchannels on the channel size and on the ionic concentration of the liquid.

The additional flow resistance in the microchannels can also be seen from the friction coefficient. The friction coefficient C_f is the product of the friction factor f and the Reynolds number Re, i.e., $C_f = f^*Re$. It is well known that, for a macroscopic rectangular channel, the friction coefficient is a constant, i.e., $C_f = 96$. Using the definition of the friction factor,

$$f = \frac{-(dP/dx)D_h}{(1/2)\rho u_{ave}^2} = \frac{-2(dP/dx)\rho D_h^3}{\mu^2 Re_{D_h}^2} \tag{24}$$

and the experimental data, the friction coefficients for both the pure water and the 10^{-4} M KCl solution in the three microchannels are plotted in Figs. 6 and 7. As seen clearly from these figures, C_f values are higher than 96.

As discussed in Section 1, because of the presence of the EDL, the pressure-driven flow induces an electrokinetic potential, the streaming potential. The streaming potential in turn will generate a conduction electrical current and hence a liquid flow opposite to the pressure-driven flow. The net result is a reduced flow rate in the pressure-driven flow direction under a given pressure drop or a higher-pressure drop for a given flow rate, in comparison with the conventional Poiseuille flow model. This is the electro-viscous effect. The flow-induced streaming potential was measured in this study.

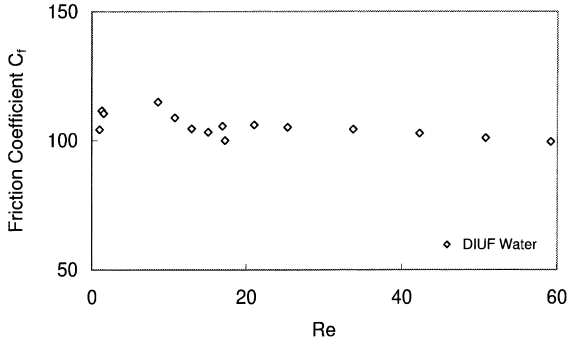

Fig. 6. Friction coefficient as a function of Reynolds number for pure water in the three microchannels.

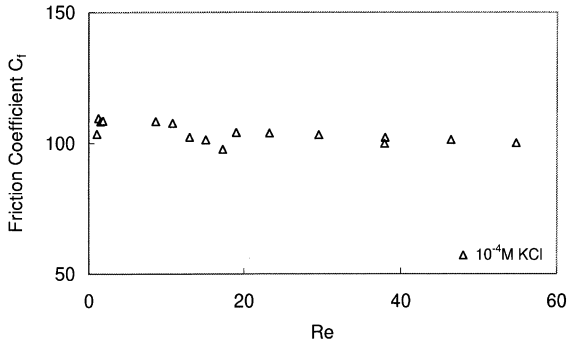

Fig. 7. Friction coefficient as a function of Reynolds number for 10^{-4} M KCl solution in the three microchannels.

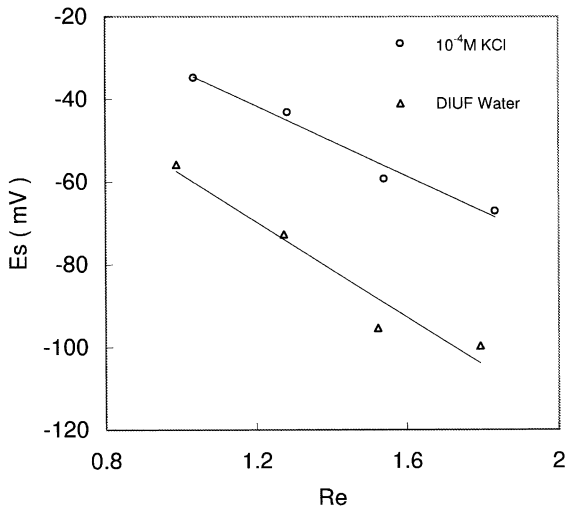

Fig. 8. Measured streaming potential and Reynolds number for a microchannel of height 14.1 μm.

Figs. 8–10 show the measured streaming potential vs. the Reynolds number for the 10^{-4} M KCl solution and the DIUF water. For the 10^{-2} M KCl solution, the streaming potential is close to zero and not plotted here. In all these figures, each point represents an average value of six independent measurements, with an error of approximately ±5%. As seen from these figures, for a given liquid, the absolute value of streaming potential increases as the *Re* increases. This is simply because the flow-induced streaming potential increases with the flow. It is also clearly seen from these figures that the absolute value of the streaming potential of DIUF water is always higher than that of the 10^{-4} M KCl solution. A larger streaming potential corresponds to a stronger

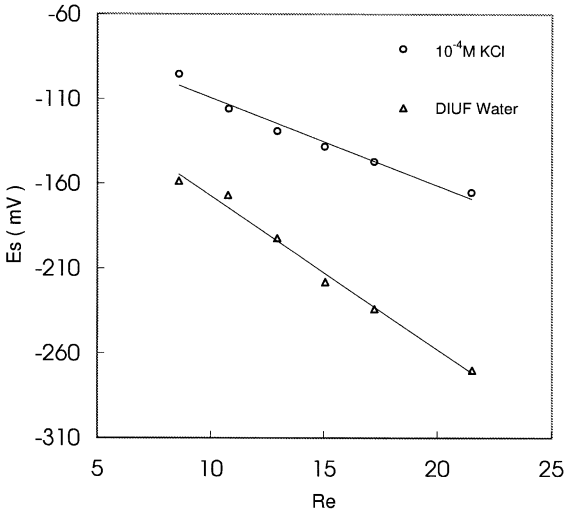

Fig. 9. Measured streaming potential and Reynolds number for a microchannel of height 28.2 μm.

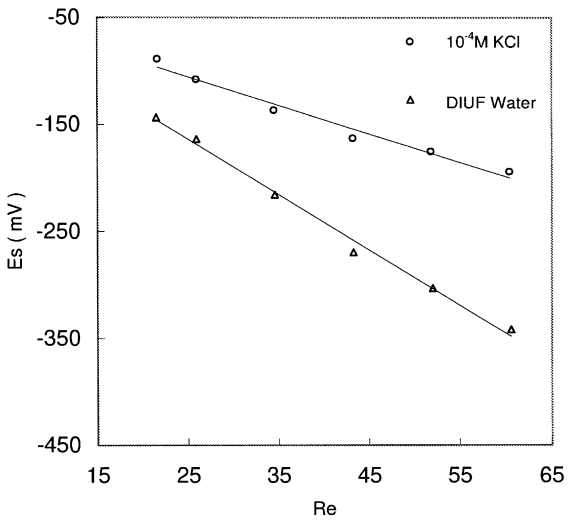

Fig. 10. Measured streaming potential and Reynolds number for a microchannel of height 40.5 μm.

electro-viscous effect. Therefore, these experimental evidences confirm the significant electro-viscous effect on the flow behavior of aqueous solutions of low ionic concentrations in small microchannels.

In the theory of electrokinetics [17], the streaming potential E_x and the pressure drop ΔP across a slit capillary channel are related to the Zeta potential ς through the following equation

$$\frac{E_x}{\Delta P} = \frac{\varepsilon \varsigma}{\mu(\lambda_0 + \lambda_s/H)}, \tag{25}$$

where λ_0 is the electrical conductivity of the liquid, λ_s the surface conductance, ε and μ the dielectric constant and viscosity of the liquid, and H is the half of the channel height. Using the measured streaming potential and the measured pressure drop for different channel heights, the Zeta potential and the surface conductance can be determined by using this equation. The detailed procedures can be found elsewhere [17]. The Zeta potentials are approximately 276 mV for the silicon surface with DIUF water and 107 mV for the silicon surface with the 10^{-4} M KCl solution, respectively.

In this study, the electrokinetic flow model, Eqs. (10) and (20), were solved numerically. The model predictions were compared with the experimental data, as shown in Figs. 11–13. In all these figures, the solid lines for the 10^{-2} M solution were predicted by the conventional Poiseuille laminar flow model. Clearly, it agrees well with the experimental data, indicating negligible EDL effect for the high ionic concentration solution. With the 14.1 μm channel, the model predicted $dP/dx \sim Re$ line for pure water agrees well with the experimental data points. For the 10^{-4} M solution, the predicted $dP/dx \sim Re$ line is lower than the experimental data points. With the 28.2 μm channel, the predicted $dP/dx \sim Re$ lines for both the pure water and the 10^{-4} M solution are lower than the experimental data points in the lower Reynolds number range. For the 40.5 μm channel, the predicted $dP/dx \sim Re$ line for the pure water agrees well with the experimental data points. Overall, the electrokinetic flow model presented in this paper can qualitatively predict the behavior of the aqueous solution flows in microchannels.

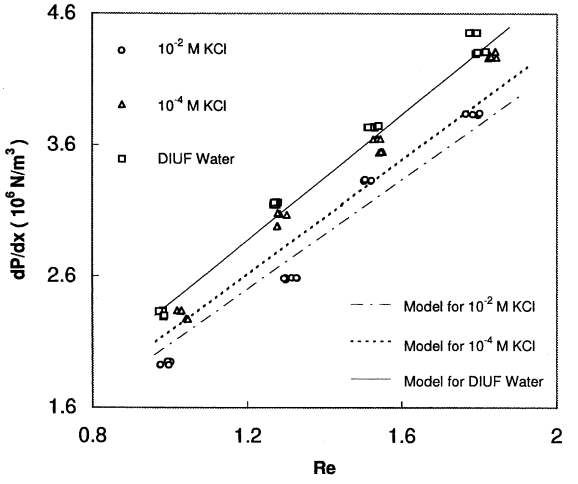

Fig. 11. Comparison of the experimentally determined $dP/dx \sim Re$ relationships with the predictions of the electro-viscous flow model for a microchannel of height 14.1 μm.

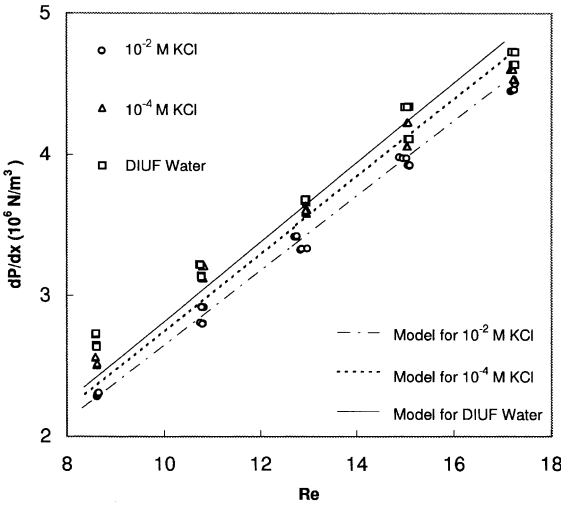

Fig. 12. Comparison of the experimentally determined $dP/dx \sim Re$ relationships with the predictions of the electro-viscous flow model for a microchannel of height 28.2 μm.

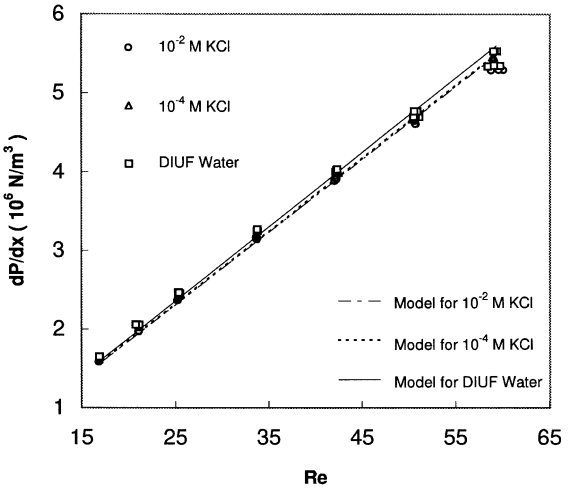

Fig. 13. Comparison of the experimentally determined $dP/dx \sim Re$ relationships with the predictions of the electro-viscous flow model for a microchannel of height 40.5 μm.

5. Summary

The correlation of pressure drop and the volume flow rate of pure water and two aqueous KCl solutions in silicon microchannels was experimentally studied. Overall, up to 20% higher flow resistance (i.e., dP/dx) was found for pure water and the low ionic concentration solution. The results show a strong dependence of $dP/dx \sim Re$ relationship on the channel size and on the ionic concentration of the liquids. The flow-induced streaming potential was also measured in this study. At the same flow rate, the pure water has the highest streaming potential, the high concentration (10^{-2} M) KCl solution has the lowest (essentially zero) streaming potential. According to the electrokinetic theory, the higher the streaming potential, the higher the electro-viscous effect on flow. These correspond well with the measured $dP/dx \sim Re$ relationship. The experimental data were compared with an electrokinetic flow model developed in this paper. The comparison confirms that the electrical double layer effect or the electro-viscous effect is the major cause of the significantly higher-pressure drop for pure water and dilute aqueous ionic solutions flowing through small microchannels.

Acknowledgements

The authors wish to acknowledge the support of a Research Grant of the Natural Science and Engineering Research Council of Canada.

References

[1] D.B. Tuckerman, R.F.W. Pease, IEEE Electron Device Lett. 2 (1981) 126.
[2] M.M. Rahman, F. Gui, Adv. Electron. Packaging 199 (4) (1993) 685.
[3] W. Urbanek, J.N. Zeemel, H.H. Hau, J. Micromech. Microeng., 3 (1993) 206.
[4] J.N. Pfahler, Liquid transport in micron and submicron size channels, Ph.D. thesis, Dept. of Mech. Eng. and Appl. Mech., Univ. of Pennsylvania, 1992.
[5] G.M. Mala, D. Li, C. Werner, H.J. Jacobasch, Y.B. Ning, Int. J. Heat Fluid Flow 18 (1997) 489.
[6] G.M. Mala, D. Li, Int. J. Heat Fluid Flow 20 (1999) 142.
[7] R.J. Hunter, Zeta Potential in Colloid Science: Principles and Applications, Academic Press, New York, 1981.
[8] D. Burgreen, F.R. Nakache, J. Phys. Chem. 68 (1964) 1084.
[9] C.L. Rice, R. Whitehead, J. Phys. Chem. 69 (1965) 4017.
[10] S. Levine, J.R. Marriott, G. Neale, N. Epstein, J. Colloid Interface Sci. 52 (1975) 136.
[11] C. Yang, D. Li, J. Colloid Interface Sci. 194 (1997) 95.
[12] C. Yang, D. Li, J.H. Masliyah, Int. J. Heat Mass Transfer 41 (1998) 4229.
[13] C. Yang, D. Li, Colloids and Surfaces A 143 (1998) 339.
[14] W. Qu, M. Mala, D. Li, Int. J. Heat Mass Transfer 43 (2000) 353.
[15] G.M. Mala, Heat transfer and fluid flow in microchannels, Ph.D. thesis, University of Alberta, 1999.
[16] C. Werner, H. Korber, R. Zimmermann, S. Dukhin, H.J. Jacobasch, J. Colloid Interface Sci. 208 (1998) 329–346.
[17] J. Lykelema, M. Minor, Colloids and Surfaces A 140 (1997) 33.